

A Novel UWB Filter with WLAN and RFID Stop-Band Rejection Characteristic using Tri-Stage Radial Loaded Stub Resonators

Chengyuan Liu, Tao Jiang, Yingsong Li, and Jing Zhang

College of Information and Communications Engineering,
Harbin Engineering University, Harbin, Heilongjiang, 150001, China
liuchengyuan@hrbeu.edu.cn, liyingsong@hrbeu.edu.cn

Abstract — The paper presents a novel approach for designing compact ultra-wideband (UWB) band-pass filter with WLAN and RFID stop-band rejection characteristic which is obtained by using tri-stage radial loaded stub resonators. The main advantage of the proposed filter is that the Stop-band can perfectly reject the WLAN and RFID (5.2GHz-6.1GHz) signals. The density and the equivalent model of one filter for testing the presented design is given depending on the odd/even excitation resonance condition. The characteristics of the filter are analyzed and discussed. To verify the proposed methods, two filters are designed and fabricated. Measured results show the proposed UWB properties from 3 GHz to 10.8 GHz and stop-band properties from 5.2 GHz to 6.1GHz. The designed filters can be integrated in UWB radio systems and can efficiently enhance the interference immunity from undesired signals such as wireless local area network (WLAN) and RFID.

Index Terms - Band-pass filter, dual-band, tri-stage radial loaded stub resonator, UWB, WLAN and RFID stop-band rejection

I. INTRODUCTION

Since the Federal Communications Commission (FCC) released the frequency band from 3.1GHz to 10.6 GHz for commercial applications in February 2002, the ultra-wideband (UWB) radio system has been receiving great attention from both academy and industry [1]. UWB bandpass filter (BPF) is one of the key passive components to implement UWB radio systems. Therefore, more requirements have been

proposed on the design methodology of BPFs with large fractional bandwidths (FBWs). Recently, a few methods and structures have been presented to develop UWB BPFs [2]-[5]. Generally, typical structures include a low and high-pass filter configuration [2], coplanar waveguide (CPW) [3], Right/Left-Handed Structure [4], microstrip fork-form resonators [5], split-ring resonators [6], circular slots in ground plane [7], multi-mode resonators (MMR) [8]. Though most of the UWB BPFs are suitable for application, they have some imperfections, such as bad out-of-band performance and complex structure.

Moreover, the UWB frequency band overlaps with some existing telecommunication bands such as WLAN RFID and WiMAX which indicate that they may interfere with UWB systems and vice versa. Therefore, a compact communication system which operates in UWB frequency band requires two types of filters. The first is a small BPF with a notched band (bandwidth is less than 150MHz.) in order to avoid being interfered by the undesired radio signals. The second is a compact BPF with stop-band rejection characteristic in order to avoid being interfered by the undesired radio signals and to get good UWB signal. Recently, there are many methods that have been investigated to design filters for the first kind with a notched band, such as embedded open-circuited stub [9], defected ground structures (DGS) [10], mismatch transmission line [11], Tri-layer structure [12], open-loop structure [13], E-shaped Microstrip SIR [14], surface-coupled structure [15] and parasitic coupled line [16] which can effectively isolate undesired radio signals. For the second kind UWB filter, there are not effective ways to complete this design. Because general

structures cannot achieve stop-band rejection characteristic near 1GHz (5.2GHz-6.1GHz). Several methods have been developed and investigated for designing this kind of filters [17-18]. However, these structures are difficult in integrating into UWB filter.

The present paper provides a new implementation of stop-band rejection characteristic by using tri-stage radial loaded stub resonators. The tri-stage radial loaded stub resonators is designed based on the loaded stub resonator. The loaded stub resonator has a good dual-mode resonance characteristic which is widely used to design dual-band UWB bandpass filter [19-20]. Different with the general dual-band filter designed, in this article we use tri-stage radial loaded stub resonators to get WLAN and RFID stop-band rejection characteristic. The tri-stage radial loaded stub resonator also has good dual-mode characteristic. The odd mode resonance is used to design the UWB filter. At the same time, the even mode resonance is regarded as a band reject block. By changing the tri-stage radial loaded stub resonator, the odd mode is hardly changed. So the frequency of the stop-band can alter optionally to reject different signals. Furthermore, the width of the stop-band could be expanded by adjusting the length of the middle stage radial loaded stub. The filter performance is simulated by using the CST software and it is implemented on the substrate with a relative dielectric constant of 10.8 and a thickness of 0.635 mm. Simulated and measured results agree reasonably well.

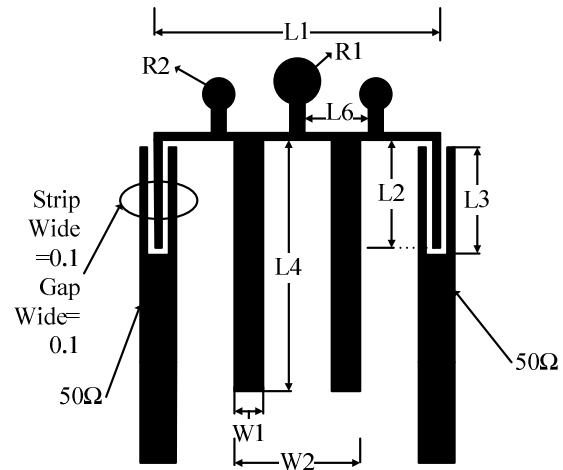
II. FILTER DESIGN AND ANALYSIS

In this Section, the theoretical design and synthesis of a compact UWB BPF with stop-band rejection characteristic using dual-/tri-stage radial loaded stub resonators is presented. The proposed filter design essentially exploits the dual-/tri-stage radial loaded stub structures for the realization of good WLAN and RFID stop-band rejection characteristic. This section is organized as follows. Section 2.1 outlines the characteristics of the compact UWB BPF with good WLAN and RFID stop-band rejection characteristic using dual-stage radial loaded stub. In addition, the corresponding lumped equivalent circuits and formulas are provided. But this method still has a little disadvantage such as narrow bandwidth of stop-

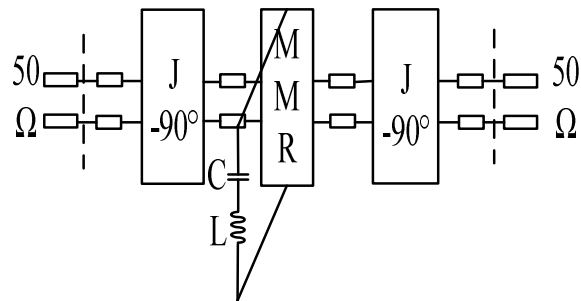
band rejection characteristic. To overcome that problem, we use the tri-stage radial loaded stub to substitute for dual-stage radial loaded stub. The modified filter using tri-stage radial loaded stub is described in section B.

A. UWB BPF with Stop-band characteristic using Dual-stage radial loaded stub

The schematic and equivalent transmission line model of the investigated UWB BPF with wide stop-band rejection is shown in Fig. 1.



(a) The layout,



(b) equivalent circuit network of the filter,

Fig. 1 Geometry of the proposed UWB filter using dual-stage radial loaded stub.

The proposed UWB filter consists of stubs-loaded MMR at the center section and two identical coupled-lines located at the left and right section. The proposed BPF is a modified form of [8] and the dual-stage radial loaded stub is coupled to the middle MMR section to achieve the stop-band rejection characteristic. Fig. 1 (b) illustrates the equivalent transmission line network of the proposed filter. The inter-digital coupled line can be

equaled as two single transmission lines at two sides and a J-inverter susceptance in the middle. This MMR is formed by attaching three round stubs in the middle section. They can work together to produce an extended stop-band in the higher frequency range. On the other hand, the middle section of the constituted MMR also exhibits an excellent low-pass property with sharpened rejection skirt.

The dual-stage radial loaded stub inserted into the middle section of the MMR can be seen as a shunt series resonant branch. This branch is regarded as a capacitor and cascade inductors. The dual-stage radial loaded stub is designed based on the radial-UIR loaded stub. The detailed analysis of radial-UIR loaded stub could be found in our previous study [21]. The radial-UIR loaded stub's equivalent model can be seen shown in Fig. 2.

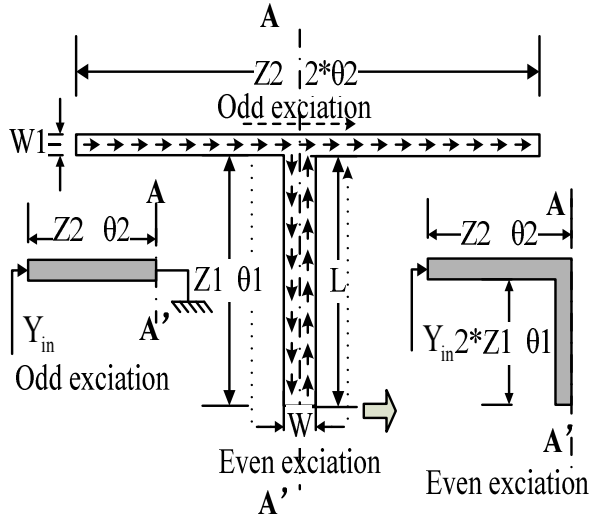


Fig. 2 equivalent mode diagram of the radial-UIR loaded stub.

From Fig. 2, the radial-UIR loaded stub can be analyzed in terms of even and odd mode (the AA' plane behaves as an electric/magnetic wall for odd/even mode). For odd mode, the center UIR has no influence on the electrical response while the radial-UIR loaded stub is relevant to even mode response. The even mode excitation condition can be extracted from resonant condition is expressed as follows [22]:

$$Y_{in} = jY_2^*$$

$$\frac{2(R_z \tan \theta_1 + \tan \theta_2)(R_z - \tan \theta_1 \tan \theta_2)}{R_z(1 - \tan^2 \theta_1)(1 - \tan^2 \theta_2) - 2(1 - R_z^2) \tan \theta_1 \tan \theta_2},$$

$$R_z = \frac{Z_2}{Z_1}. \text{ Resonant conditions are obtained by}$$

taking $Y_{in} = 0$. Thus we can get

$$(R_z \cot \theta_2 + \cot \theta_1)(R_z \cot \theta_1 \cot \theta_2 - 1) = 0.$$

In this filter $Z_2 = 90\Omega$, $\theta_2 = 90^\circ$ and $Z_1 = 72\Omega$. So we can get $\theta_1 = 90^\circ$. Then the length of the stub is designed near $\lambda_{notch} / 4$ which is illustrated as follows:

$$\lambda_{notch} = \frac{C}{f_{notch} \sqrt{\epsilon_{eff}}},$$

$$\epsilon_{eff} = \sqrt{\frac{\epsilon_r + 1}{2}},$$

where λ_{notch} is the wavelength of the center frequency of the notch band, f_{notch} is the center frequency of the notch band, ϵ_r is the relative dielectric constant, ϵ_{eff} is the effective dielectric constant, and C is the speed of light.

In this paper, we want to get a wide stop-band rejection characteristic. From [19], we know that the width of the radial-UIR loaded stub can control the width of the stop-band. The effects of the wide stop-band characteristic has been investigated. Fig. 3 shows the response $|S_{21}|$ of the mentioned filter with various W . By increasing the width of radial-UIR loaded stub, the width of the stop-band is changed.

From Fig. 3, it is clear that the bandwidth of the stop-band increases to the wider level with the increase of W . More specifically, the width of the stop-band (-20dB) would increase to near 1GHz

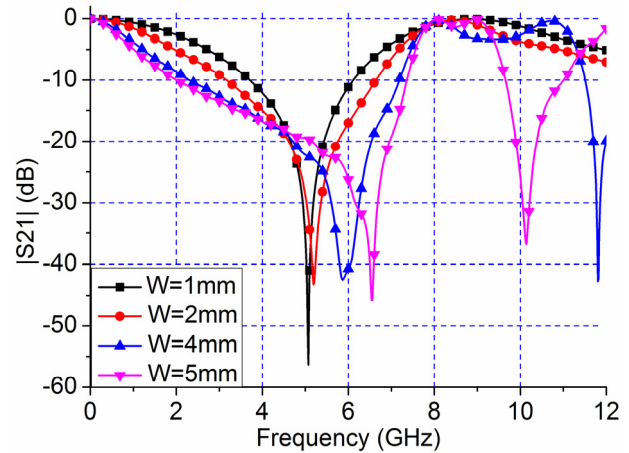


Fig. 3 Simulated $|S_{21}|$ of the stub for different W with other parameter fixed.

when the width of the stub is increased to 4mm. Although this method could obtain enough bandwidth of the stop-band, there is a very poor rectangular coefficient. In addition, there would be a spurious frequency from 10GHz to 14GHz. The spurious frequency could influence the pass-band of UWB filter. In another case, the width of the stub (W) is far greater than the width of branch ($W1$). So discontinuities in the transmission-line should be taken into consideration. This will increase the difficulty of accurate design.

To overcome that problem, we should use other structures to substitute for general radial-loaded stub. At first, we analyze the current density of the proposed general radial-loaded stub. Figure 4 shows the current density of the general stub at the frequency of pass-band and at the stop-band frequency.

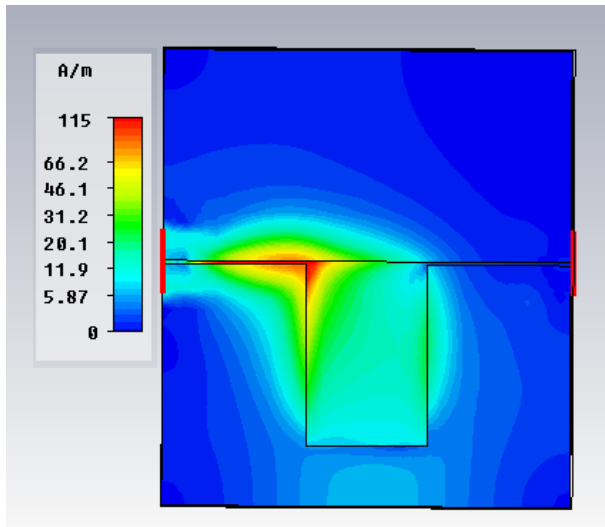


Fig. 4 Current density of the general stub at the stop-band frequency ($f=6\text{GHz}$).

It can be seen from the current density of the structure in the pass-band frequency that the stub does not resonate and has no effect on the overall performance. At the stop-band frequency ($f=6\text{GHz}$), the stub resonates with a much higher current density along the two edges of the general radial-loaded stub. At the same time, we can clearly see that the middle of the stub has lower current density. By cutting out the lower current density part and retain the higher current density part, we could get degenerate radial loaded stub (dual-stage radial loaded stub). By using this method, we could obtain

reasonable current distribution. The (the ratio of $W/W1$) discontinuities of this structure is also reduced at the same time.

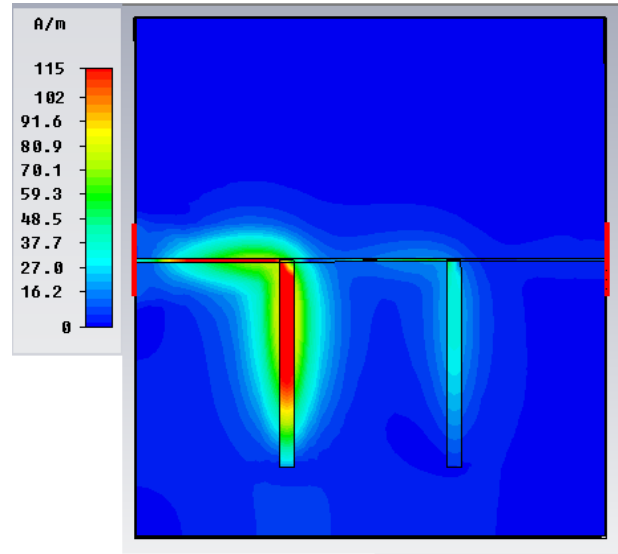


Fig. 5 Current density of the dual-stage radial loaded stub at the stop-band frequency ($f=6\text{GHz}$).

From Fig. 5, it can be seen clearly that the degenerated radial loaded stub (dual-stage radial loaded stub) could achieve the function of the general stub well. Next, we compare the simulation results of the two kinds of stubs to verify the effectiveness of the method further.

It can be seen from Fig. 6 that good wide stop-band rejection has been achieved by using the dual-stage radial loaded stub. From the comparison

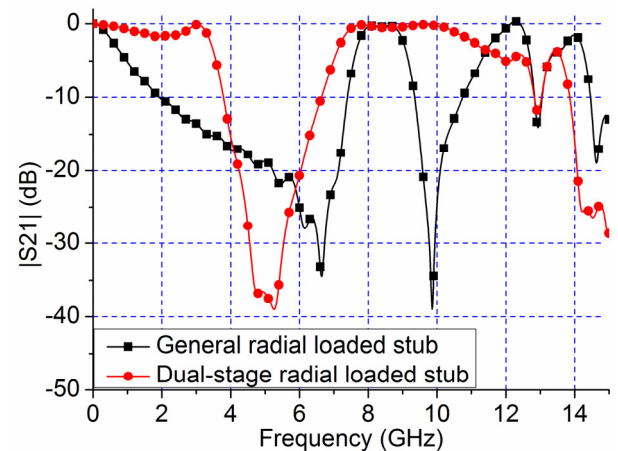


Fig. 6 Comparison of simulated $|S_{21}|$ of Dual-stage stub and general stub.

of simulated $|S_{21}|$ of the dual-stage stub and general stub, we can see that dual-stage stub can generate good rectangular coefficient and reject spurious frequency response at the same time. Figure 7 shows response $|S_{21}|$ of the mentioned filter with various L_4 .

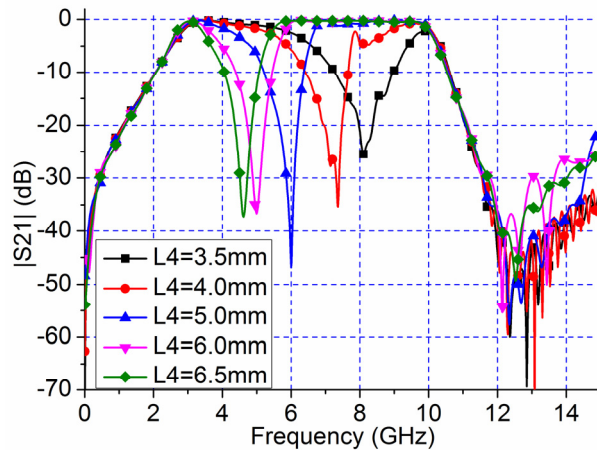


Fig. 7 Simulated $|S_{21}|$ of the proposed filter in Fig. 1 for different L_4 with other parameter fixed.

Form Fig. 7, it is found that the center frequency of the stop-band shifts to the lower level with the increase of L_4 . However, the filter can always maintain nearly 500 MHz of bandwidth within stop-band. Because the dual-stage radial loaded stub resonator is a degenerated form of general stub, so this structure inherited the advantages of the original structure. The frequency of the stop-band can be easily controlled by adjusting the dimensions of the dual-stage radial loaded stub resonator. More specifically, the filter could block undesired existed radio signals (except WLAN and RFID) from UWB communication. Although the dual-stage radial loaded stub resonator can get a good stop-band rejection characteristic, it is still not convenient for the design via limited design parameters. On the other hand, the rectangular coefficients of dual-stage radial loaded stub are not good enough from the Fig. 7. To overcome that problem, we substitute the tri-stage radial loaded stub for the dual-stage radial loaded stub.

B. UWB BPF with stop-band characteristic using Tri-stage radial loaded stub resonator

Compared with the dual-stage radial loaded stub resonator, tri-stage radial loaded stub resonator

has a wider degree of the freedom in structure and design. The schematic of the proposed filter using tri-stage radial loaded stub is shown in Fig. 8.

Compared with the designed filter in Fig. 1, the difference is the inner stub. The additional stub can bring extra resonant frequency and expand the stop-band bandwidth. Comparison of simulated $|S_{21}|$ of these mentioned two filters is shown in Fig. 9. From the Fig. 9, it is clear to see that if the middle stub is added, the width of stop-band would be twice of that of the dual-stage radial loaded stub. In order to get more detailed research results, the UWB filter using tri-stage radial loaded stub resonator is analyzed using CST and discussed herein. Figures 10 and 11 show the filter response $|S_{21}|$ of with varying L_5 ($L_5 < 5\text{mm}$ and $L_5 > 5\text{mm}$).

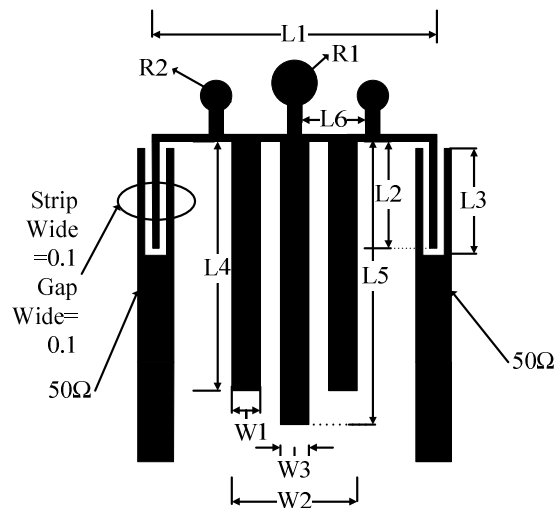


Fig. 8 Geometry of the proposed UWB filter using tri-stage radial loaded stub.

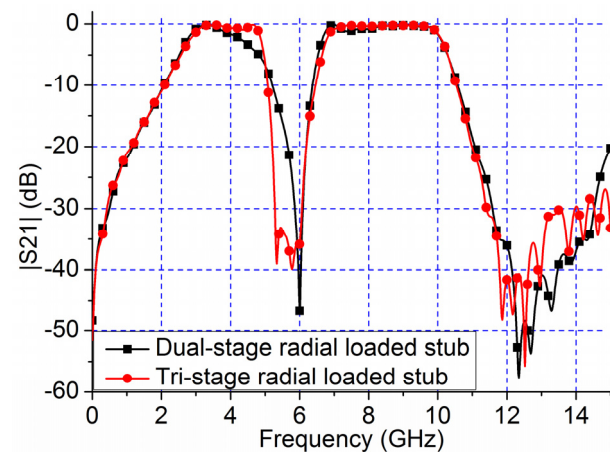


Fig. 9 Comparison of simulated $|S_{21}|$ of these mentioned two filters.

There have one point need to be noted is that when $L_4=L_5=5\text{mm}$, the bandwidth of stop-band is the same as using the dual-stage radial loaded stub. This is because of that the tri-stage radial loaded stub could be seen as degenerated radial loaded stub when $L_4=L_5=5\text{mm}$.

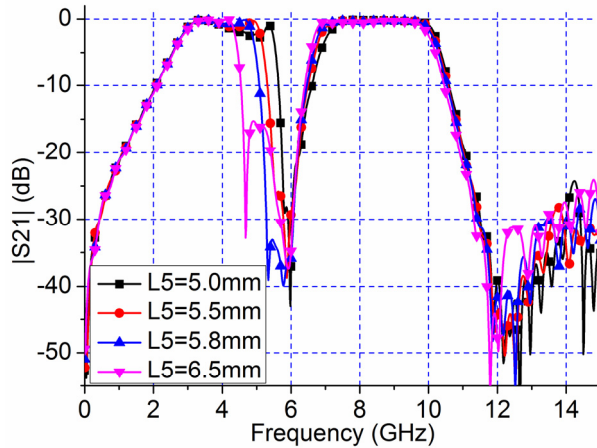


Fig. 10 Simulated $|S_{21}|$ of the proposed filter for different L_5 with other parameter fixed ($L_5 > 5\text{mm}$).

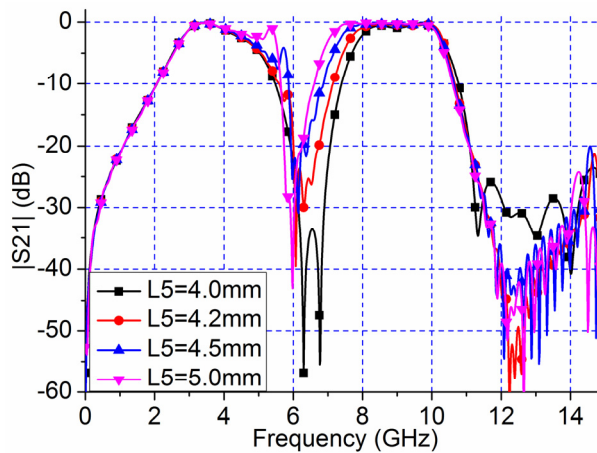


Fig. 11 Simulated $|S_{21}|$ of the proposed filter for different L_5 with other parameter fixed ($L_5 < 5\text{mm}$).

From the Fig. 10, it is clear to see that if the middle stub L_5 increases (L_5), the stop-band would expand to a lower level. In other words, an increase of L_5 can expand the stop-band to the lower level. Furthermore we could see that the middle stub brings out an additional frequency. When the additional frequency moved to the lower, the stop-band could expand to near 1GHz. It's worth noting

that the stop-band would be distorted with $L_5=6.5\text{mm}$.

From Fig. 11, it is clear to see that if the middle stub L_5 decreases (L_5), the stop-band could expand to a higher level. In other words, a decrease of L_5 could expand the stop-band to a higher level. As the same as Fig. 10, the middle stub brings out an additional resonance frequency. When the additional frequency moves to a higher level, the stop-band also expands to near 1GHz. Based on the above discussions, the resonance frequency of the stop-band can be easily controlled by adjusting the dimensions of the dual/tri-stage radial loaded stub. More specifically, the filter using dual-stage radial loaded stub could block most undesired existed radio signal (except WLAN and RFID) within the UWB operation band. The filter using tri-stage radial loaded stub could block all undesired existed radio signals within UWB communication.

Based on the above parametric study, the proposed filter is optimized and manufactured after several adjustments of different parameters. Figure 12 and Fig. 13 shows the simulated results of different L_3 and W_3 . According to the details of Fig. 12 and Fig. 13, the optimal dimensions can be determined. The final dimensions of the designed filter are as follows: $L_1=6.4\text{mm}$, $L_2=3.7\text{mm}$, $L_3=4\text{mm}$, $L_4=6\text{mm}$, $L_5=1.8\text{mm}$, $L_6=1.5\text{mm}$, $R_1=0.6\text{mm}$, $R_2=0.5\text{mm}$, $W_1=0.1\text{mm}$, $W_2=1\text{mm}$.

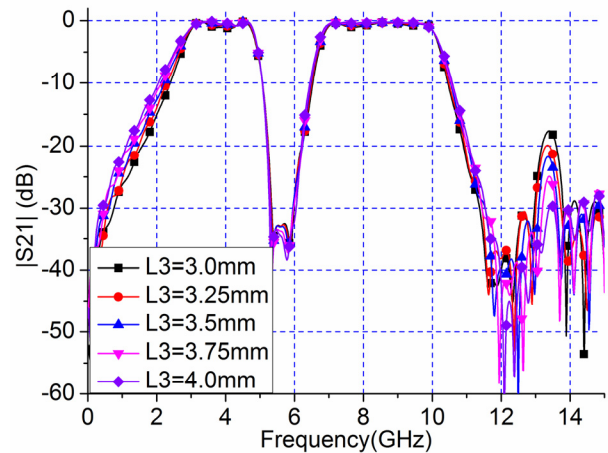


Fig. 12 Simulated $|S_{21}|$ of the proposed filter for different L_3 .

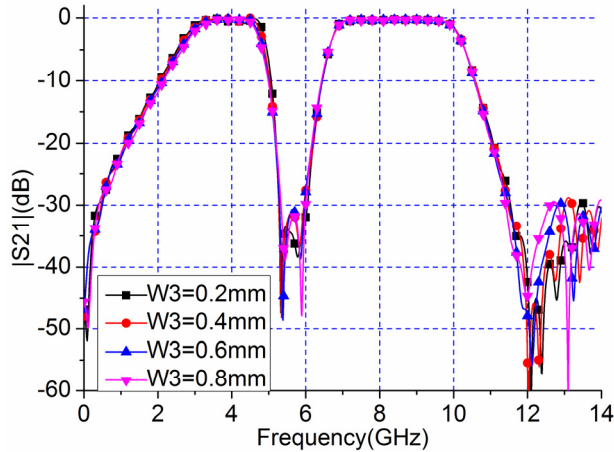


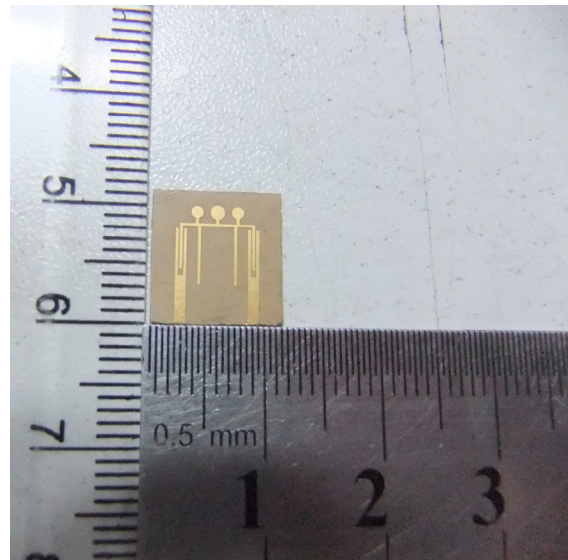
Fig. 13 Simulated $|S_{21}|$ of the proposed filter for different W_3 .

III. EXPERIMENTAL RESULT

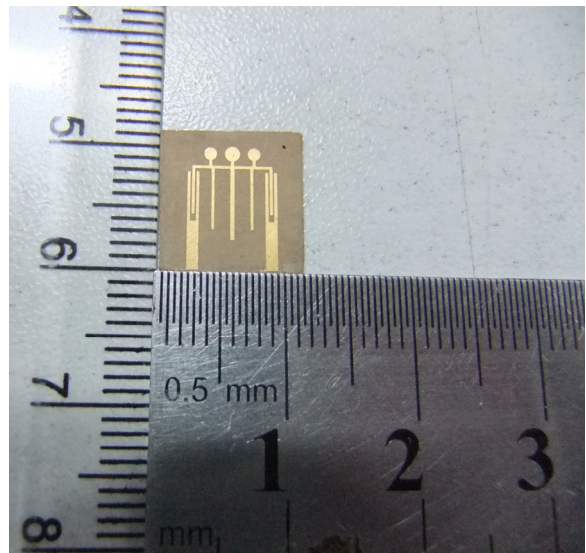
To verify the effectiveness of the proposed filters, the proposed dual-wideband BPFs with stop-band rejection characteristic using dual/tri-stage radial loaded stub resonators are designed, simulated, fabricated and measured. To compare the difference of the two designs, basic parameters of the two filters are the same. Figure 14 is the photograph of the fabricated filters. The overall circuit size of these filters are less than $10\text{mm} \times 10\text{mm}$, so these filters are compact.

The proposed dual-wideband BPFs with wide stop-band rejection characteristic using dual/tri-stage radial loaded stub is measured by Anristu 37347D vector network analyzer. Figure 15, Fig. 16, Fig. 17 and Fig. 18 demonstrate the frequency responses and group delay of proposed filters. The excellent agreement is obtained when compared with simulated ones. Both of the simulation and modified filter using dual-stage radial-loaded stub. Measured results of the two filters show that the two filters have two pass bands and a stop-band rejection characteristic. Form Fig. 15, the first one is a filter whose center frequency is 6GHz, -3dB fractional bandwidths are 3.1GHz-4.2GHz and 6.5GHz-10.6GHz and -20dB fractional stop-band bandwidths is 5.6-6.2GHz (591MHz). The second one, shown in the Fig. 17, is a filter whose center frequency is 5.6 GHz, -3dB fractional bandwidths are 3.1GHz-4.86GHz and 6.76GHz-10.6GHz and -20dB fractional stop-band bandwidths is 5.2GHz-6.2GHz (1GHz). The only difference of the two filters is that we substituted the tri-stage radial

loaded stub for the dual-stage radial loaded stub when the second filter was designed. So we expanded the bandwidth of the stop-band to the higher level. The changing trends of the stop-band show that the filter using tri-stage radial loaded stub can improve rectangular coefficient effectively comparing to the dual-stage radial loaded stub. Because the tri-stage radial loaded stub add a parameter, which made the modified filter have a wide degree of the freedom in structure and design.



(a) filter using dual-stage radial loaded stub,



(b) filter using tri-stage radial loaded stub

Fig. 14 Phototype and of the fabricated filter.

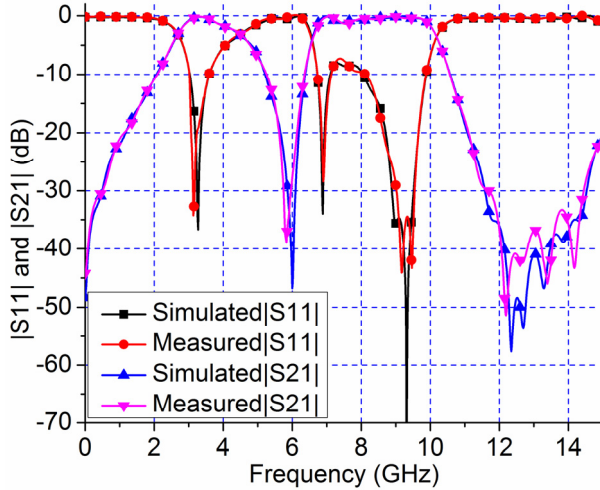


Fig. 15 Comparison of simulated and measured $|S_{11}|$ and $|S_{21}|$ using dual-stage radial-loaded stub.

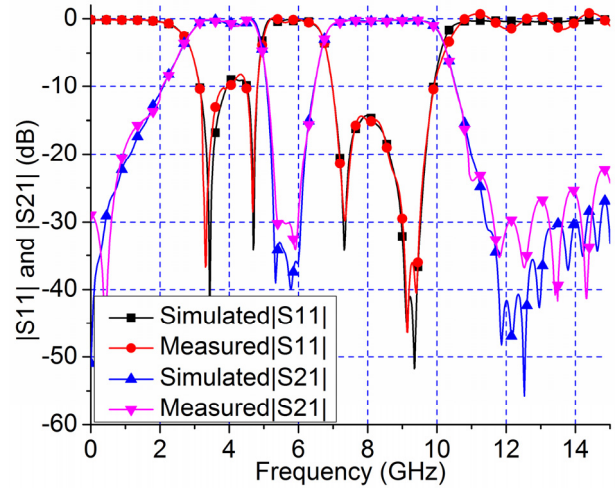


Fig. 17 Comparison of simulated and measured $|S_{11}|$ and $|S_{21}|$ using Tri-stage radial-loaded stub.

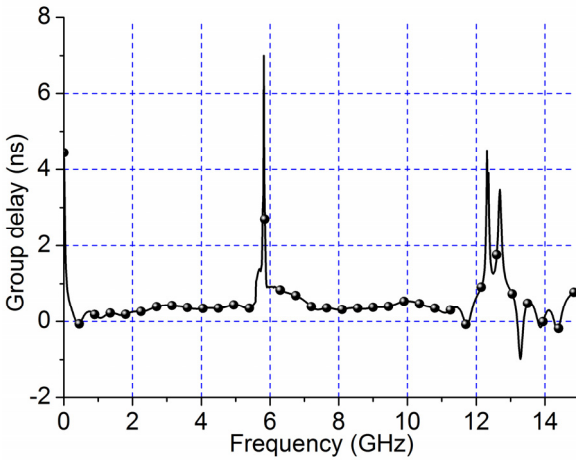


Fig. 16 Measured group delay of the fabricated.

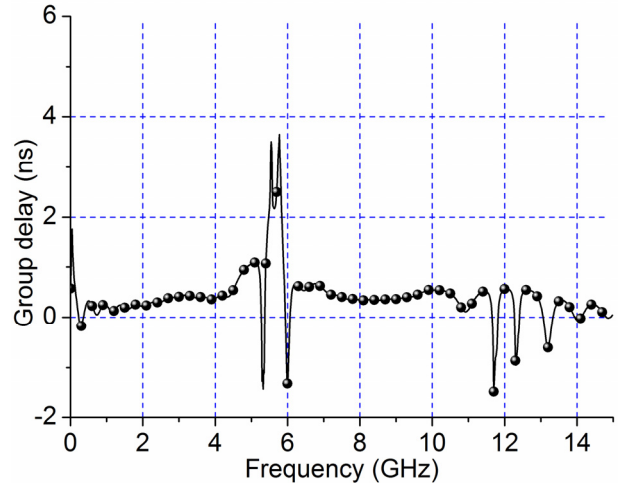


Fig. 18 measured group delay of the fabricated modified filter using Tri-stage radial-loaded stub.

The simulated and measured results show good agreement. This minor discrepancy between simulated and measured results should be caused by insertion loss of SMA connectors and unexpected tolerances in fabrication, material parameters and solder etc. As shown in Fig. 15 and Fig. 17 the measured insertion loss is less than 0.5dB. The rejection between the two transmission bands is more than 25 dB. As shown in Fig. 16 and Fig. 18, the measured group delay is between 0.2ns and 0.6 ns with a maximum variation of 0.6 ns in the two pass-band and more than 2ns in the middle stop-band. At upper rejection band, the presented filters have deeper and wider stop-band attenuation which is more than -25 dB from 11 to 15 GHz.

It should be noted that the filters are embarrassed in that the return loss is quite high in the first pass-band since three round stubs of the origin structure [8] are cut by the filters to get enough space to design, which would reduce the strength of the resonance. So the insertion loss would have some attenuation. However, in this structure, the gap and size are so small that the attenuation can be controlled in an acceptable range. At the same time, the attenuation of the filters in the pass-band is nearly constant. Based on the above analysis, although the two filters have little defect, they are still good UWB filters with notch-band character. Simualed and

measured results show that the two filters are good ultra-wide notch-band BPFs, which can be suitable for implementing the functions of UWB system.

IV. CONCLUSION

In this paper, two compact UWB BPFs with WLAN and RFID stop-band rejection characteristic have been developed and manufactured. Inserting dual/tri-stage radial loaded stub to the original UWB BPF leads to rejection of undesired existed radio signals such as wireless local area network (WLAN) and RFID. The dual/tri-stage radial loaded stub can bring out a stop-band rejection characteristic at the desired frequency with no significant influence on the wide passband performance of the filter. In particular, changing the length of the dual-stage radial loaded stub can adjust the stop-band optionally in a wide range. Changing the length of the third-stage radial loaded stub can expand the bandwidth of stop-band to 1GHz for perfect WLAN and RFID stop-band rejection characteristic. The proposed filters are promising for use in UWB systems due to their simple structures, compact size, and excellent performance.

ACKNOWLEDGMENT

This work was supported by a grant from the National Defense "973" Basic Research Development Program of China (No.6131380101), the National Nature Science Fund of China (No.60902014), Nature Science Fund of Heilongjiang (No.2006F11), Core Young Teacher Fund of Harbin Engineering University (No.0812) and Fundamental Research Funds for the Central Universities (HEUCF1208).

REFERENCES

- [1] FCC, Revision of Part 15, *the Commission's Rules Regarding to Ultra-Wide-Band Transmission System, First Note and Order Federal Communication Commission*, ET-Docket pp. 98-153, 2002.
- [2] C. L. Hsu, F. C. Hsu, and J. T. Kuo, "Microstrip Bandpass Filters for Ultra-Wideband (UWB) Wireless Communications", *2005 IEEE MTT-S International Microwave Symposium Digest*, pp. 679-682, 2005.
- [3] H. Wang, L. Zhu, and W. Menzel, "Ultra-Wideband Bandpass Filter with Hybrid Microstrip/CPW Structure", *IEEE Microwave Wireless Compon Lett.*, vol. 15, pp. 844-846, 2005.
- [4] J. Q. Huang and Q. X. Chu, "Compact UWB Band-Pass Filter Utilizing Modified Composite Right/Left-Handed Structure with Cross Coupling," *Progress In Electromagnetics Research*, vol. 107, pp. 179-186, 2010.
- [5] H. Chen and Y. X. Zhang, "A Novel and Compact UWB Bandpass Filter using Microstrip Fork-Form Resonators," *Progress In Electromagnetics Research*, vol. 77, pp. 273-280, 2007.
- [6] L. Qiang, Y. J. Zhao, Q. Sun, W. Zhao, and B. Liu, "A Compact UWB Bandpass Filter based on Complementary Split-Ring Resonators," *Progress In Electromagnetics Research C*, vol. 11, pp. 237-243, 2009.
- [7] M. NaghshvarianJahromi and M. Tayarani, "Miniature Planar UWB Bandpass Filters with Circular Slots in Ground," *Progress In Electromagnetics Research Letters*, vol. 3, pp. 87-93, 2008.
- [8] B. Yao, Y. Zhou, Q. Cao, and Y. Chen, "Compact UWB Bandpass Filter With Improved Upper-Stopband Performance", *IEEE Microwave and Wireless Components Lett.*, vol. 19, pp. 27-29, 2009.
- [9] H. Shaman and J. S. Hong, "Ultra-Wideband (UWB) Bandpass Filter with Embedded Band Notch Structures," *IEEE Microw. Wireless Compon Lett.*, vol. 17, pp. 193-195, 2007.
- [10] L. Chen, Y. Shang, and Y. L. Zhang, "Design of a UWB Bandpass Filter with a Notched Band and Wide Stopband," *Microwave Journal*, vol. 52, pp. 96-105, 2009.
- [11] T. Jiang, C. Y. Liu, Y. S. Li, and M. Y. Zhu, "Research on a Novel Microstrip UWB Notch-Band BPF," *Asia Pacific Microwave Conference*, pp. 261-264, 2009.
- [12] P. Y. Hsiao and R. M. Weng, "Compact Tri-layer Ultra-wideband Bandpass Filter with Dual Notch Bands," *Progress In Electromagnetics Research*, vol. 106, pp. 49-60, 2010.
- [13] P. Y. Hsiao and R. M. Weng, "Compact Open-loop UWB Filter with Notched Band," *Progress In Electromagnetics Research Letters*, vol. 7, pp. 149-159, 2009.
- [14] Y. L. Wu, C. Liao, and X. Z. Xiong, "A Dual-Wideband Bandpass Filter based on E-shaped Microstrip SIR with Improved Upperstopband Performance," *Progress In Electromagnetics Research*, vol. 108, pp. 141-153, 2010.
- [15] J. Q. Huang, Q. X. Chu, and C. Y. Liu, "Compact UWB Filter based on Surface-coupled Structure with Dual Notch Bands," *Progress In Electromagnetics Research*, vol. 106, pp. 311-319, 2010.

- [16] S. Pirani, J. Nourinia, and C. Ghobadi, "Band-Notched UWB BPF Design Using Parasitic Coupled Line," *IEEE Microwave and Wireless Components Lett.*, vol. 20, pp. 444-446, 2010.
- [17] R. N. Baral, P. K. Singhal, "Design and Analysis of Microstrip Photonic Band Gap Filter for Suppression of Periodicity," *Applied Computational Electromagnetics Society (ACES) Journal*, vol. 25, no. 2, pp. 156-159, Feb. 2010.
- [18] A. Boutejdar, M. Challal, A. Azrar, "A Novel Band-Stop Filter using Octagonal-Shaped Patterned Ground Structures along with Interdigital and Compensated Capacitors," *Applied Computational Electromagnetics Society (ACES) Journal*, vol. 26, no. 4, pp. 312-318, April 2011.
- [19] L. Zhang, Z. Y. Yu, and S. G. Mo, "Novel Plane Multimode Bandpass Filters with Radial-line Stubs," *Progress In Electromagnetics Research*, vol. 101, pp. 33-42, 2010.
- [20] M. D. C. Velazquez-Ahumada, J. Martel-Villagr, F. Medina, and F. Mesa, "Application of Stub Loaded Folded Stepped Impedance Resonators to Dual Band Filters," *Progress In Electromagnetics Research*, vol. 102, pp. 107-124, 2010.
- [21] C. Y. Liu, T. Jiang, Y. S. Li, A Novel UWB Filter with Notch-band Characteristic using Radial-UIR/SIR Loaded Stub Resonators, *Journal of Electromagnetic Waves and Applications*, vol. 25, no. 2, pp. 233-245, 2011.
- [22] Hong, J. S. and M. J. Lancaster, *Microstrip Filters for RF/Microwave Applications*, Wiley, New York, 2001.



Cheng-yuan Liu received his B.S. degree in electrical and information engineering in 2006, and M.S. degree in Electromagnetic Field and Microwave Technology from Harbin Engineering University, 2006 and 2011, respectively. Now he is a Ph.D. Candidate in Harbin Engineering University, China. He serves as receivers for the Journal of Electromagnetic Waves and Applications, Journal of Microwaves, Optoelectronics and Electromagnetic Applications, and Progress in Electromagnetics Research Series, Journal of Electromagnetic Waves and Applications. His research interests are mainly in microwave theory, UWB antenna and UWB filters.



Tao Jiang received his bachelor's degree in electrical engineering in 1994, his master's degree in information and signal processing in 1999 and his doctorate in communication and information systems in 2002 from Harbin Engineering University, China. He worked in the Harbin Institute of Technology, China as a post-doctoral fellow in 2003 and worked in the National University of Singapore as a research fellow in 2004. He is a professor in the Harbin Engineering University, China. His research interests are mainly in computational electromagnetics, microwave engineering, radio wave propagation and navigation and EMC.



Yingsong LI received his B.S. degree in electrical and information engineering in 2006, and M.S. degree in Electromagnetic Field and Microwave Technology from Harbin Engineering University, 2006 and 2011, respectively. Now he is a Ph.D. Candidate in Harbin Engineering University, China. He is a student member of Chinese Institute of Electronics (CIE), IEEE, IEICE and The Applied Computational Electromagnetics Society (ACES). He serves as receivers for the journals IEEE Antennas and Wireless Propagation Letters, Electronics Letters, International Journal of Electronics, Progress in Electromagnetics Research Series, Journal of Electromagnetic Waves and Applications, Applied Computational Electromagnetics Society Journal and COMPEL: The International Journal for Computation and Mathematics in Electrical and Electronic Engineering. His recent research interests are mainly in microwave theory, microwave and millimeter-wave circuits, small antenna technologies and computational electromagnetic.



Jing Zhang received her B.S. degree in electrical and information engineering in 2008, and M.S. degree in Signal and information processing from Harbin Engineering University, 2008 and 2011, respectively. Now she is a Ph.D. Candidate in Harbin Engineering University, China. His research interests are mainly in radar signal processing and UWB antenna and UWB filters.